Stimulated Brillouin scattering of electromagnetic waves in magnetized semiconductor plasmas

M. Salimullah, T. Ferdousi, and F. Majid
Department of Physics, Jahangirnagar University, Savar, Dhaka, Bangladesh
(Received 15 March 1994; revised manuscript received 12 July 1994)

The phenomenon of stimulated Brillouin scattering of a large-amplitude electromagnetic wave by the electron acoustic wave has been analytically investigated in a piezoelectric semiconductor plasma in the presence of an external uniform magnetic field. The Boltzmann equation with a Krook model for the collisional term has been solved in the guiding center coordinates for the nonlinear response of the plasma electrons. It is noticed that the magnetic field enhances the growth rate of the parametric instability in contrast with the fluid-model results.

I. INTRODUCTION

There has been an increasing interest in the interaction of eletromagnetic waves in solid state plasmas, viz., metals, semimetals, and semiconductors in recent years.[1–6] Microwave techniques are used for the diagnostics and other studies of optical properties of these systems. At large amplitudes of the incident electromagnetic waves, a number of nonlinear mode-coupling interactions may take place which modify the electrical and optical properties of solid-state plasmas.[7–10] A number of workers[11–17] have studied the nonlinear interaction of large-amplitude electromagnetic waves in semiconductor plasmas.

In an n-type InSb sample, the temperature of the massive doping centers can be taken to be zero ($T_i \simeq 0$). However, these doping centers are rearranged by the electron pressure, and this can form a wave pattern. This low-frequency ion-acoustic-type wave created by the thermal pressure of electrons is called the electron acoustic wave in the n-type semiconductor plasma.[18–20] In previous studies of the excitation of these electron acoustic waves in magnetized semiconductors, a hydrodynamic model of plasmas are employed for the short-wavelength perturbation mode. However, in the presence of short-wavelength perturbations due to electron acoustic modes, the fluid model of plasmas breaks down for typical parameters in magnetized semiconductors. The Larmour radius may be comparable to or even greater than the wavelength of the perturbation present in the semiconductor. Therefore, a kinetic model should be more appropriate for all these studies. We have chosen the n-InSb sample for our study because it possesses a low effective mass of electrons and, therefore, the electrons can attain high oscillatory velocities even at low pump-wave power.

In this paper we have studied the three-wave parametric instability, viz., the simulated Brillouin scattering of electromagnetic waves by a low-frequency electrostatic electron acoustic wave in a piezoelectric semiconductor in the presence of external static magnetic field. The nonlinear response for the low-frequency perturbation has been found by using the Boltzmann equation in the gyrokinetic variables.[21,22]

The paper is organized in the following way. In Sec. II, we present the kinetic model for the nonlinear response of electrons in the magnetized piezoelectric semiconductor. The Krook model for the collisional term has been assumed. The nonlinear Boltzmann equation expressed in the guiding center coordinates has been solved for the low-frequency perturbation. The nonlinearity at the high-frequency sideband has been taken through the current density. Using Poisson's equation for the electrostatic mode and wave equation for the electromagnetic sideband mode, we obtain the nonlinear dispersion relation for the low-frequency electrostatic mode in the magnetized piezoelectric semiconductor in Sec. III. Then we obtain the growth rates and threshold power density for the three-wave parametric instability viz. the stimulated Brillouin scattering in Sec. IV. Numerical results and graphical representation of them are presented in Sec. V. Finally, a brief discussion of the results is given in Sec. VI.

II. KINETIC ANALYSIS FOR THE NONLINEAR RESPONSE OF ELECTRONS

We consider a sample of n-type piezoelectric semiconductor, viz., n-InSb immersed in a uniform static magnetic field $\mathbf{B}_s = B_z\hat{\mathbf{z}}$. The semiconductor is assumed to be the source of a homogeneous and infinite plasma which is subjected to an externally driven large-amplitude electromagnetic wave (pump wave)—a high-frequency laser or a microwave—propagating in the extraordinary mode. The electric and magnetic fields of the pump wave are described by

$$\mathbf{E}_0 = \mathbf{E}_0' \exp[-i(\omega_0 t - k_0 x)] \, , \qquad \mathbf{B}_0 = c(\mathbf{k}_0 \times \mathrm{E}_0)/\omega_0 \, , \tag{1}$$

where the angular frequency ω_0 and the wave number k_0 obey the dispersion relation

$$k_0 = \frac{\omega_0}{c}\left[\epsilon_L - \frac{\omega_p^2 i(i\omega_0 - \nu_0)}{\omega_0\{\omega_c^2 + (\nu_0 - i\omega_0)^2\}}\right]^{1/2} , \tag{2}$$

where $\omega_p = (4\pi e^2 n_0^0/m)^{1/2}$ is the electron plasma fre-

0163-1829/94/50(19)/14104(8)/$06.00

quency and $\omega_c = eB_s/mc$ is the electron cyclotron frequency; $-e$, m, n_0^0, ϵ_L, ν_0, and c are the electronic charge, effective mass of the electrons, unperturbed equilibrium density of electrons, lattice dielectric constant of the semiconductor, average electron-phonon collision frequency, and the speed of light in a vacuum, respectively. Obviously, the pump wave is a mixed mode having

$$E_{0x} = -i\beta_0 E_{0y} \ , \tag{3}$$

$$\beta_0 = -\frac{\omega_p^2 \omega_c}{[\epsilon_L \omega_0 \{\omega_c^2 + (\nu_0 - i\omega_0)^2\} - i\omega_p^2(i\omega_0 - \nu_0)]} \ . \tag{4}$$

We now assume the existence of a low-frequency electrostatic short-wavelength perturbation $(\omega, \mathbf{k})$ which may be present in the semiconductor due to thermal noise or an inhomogeneity in the doping of the semiconductor. The oscillatory drift velocity of the electrons due to the pump wave and the oscillatory magnetic field of the pump wave interact parametrically with the perturbation mode $(\omega, \mathbf{k})$ and produce a high-frequency electromagnetic sideband $(\omega_1, \mathbf{k}_1; \omega_1 = \omega - \omega_0, \mathbf{k}_1 = \mathbf{k} - \mathbf{k}_0)$. This generated sideband in turn interacts with the pump wave $(\omega_0, \mathbf{k}_0)$ to produce a low-frequency ponderomotive force which amplifies and drives the low-frequency perturbation. Thus we consider the three-wave parametric decay of the pump wave into a low-frequency perturbation and a high-frequency sideband.[23]

In the phase, most studies used hydromagnetic models of semiconductor plasmas, which are sufficiently valid for the long-wavelength perturbations. However, some workers[18–20] used a fluid model of plasmas for very short-wavelength perturbation for the magnetized semiconductor plasmas. However, in these studies the Larmour radius $\rho_e = v_{\rm th}/\omega_c$, where $v_{\rm th}$ is the thermal velocity of electrons, is comparable to or even larger than the wavelength of the waves involved for the usual plasma parameters in the semiconductor plasma $(kv_{\rm th}/\omega_c \geq 1)$. The fluid model of plasmas is no longer valid for these conditions and one must employ the kinetic model of plasmas. Therefore, we describe the response of the highly collisional semiconductor plasma in the presence of external magnetic field by the Boltzmann equation expressed in the gyrokinetic variables[21,22]—the guiding center coordinates $\mathbf{x}_g$, the magnetic moment μ, the polar angle θ of the perpendicular velocity (i.e., the angle $\mathbf{v}_\perp$ makes with the x axis), and the parallel momentum p_z:

$$\frac{\partial F}{\partial t} + \dot{\mathbf{x}}_g \frac{\partial F}{\partial \mathbf{x}_g} + \dot{\mu}\frac{\partial F}{\partial \mu} + \dot{\theta}\frac{\partial F}{\partial \theta} - eE_z^T \frac{\partial F}{\partial p_z} = \left[\frac{\partial F}{\partial t}\right]_{\rm collision} , \tag{5}$$

where

$$\begin{aligned} x_g &= x - \rho \sin\theta \ , \\ y_g &= y + \rho \cos\theta \ , \\ z_g &= z \ , \\ \rho &= v_\perp/\omega_c \ , \\ \mu &= mv_\perp^2/2\omega_c \ . \end{aligned} \tag{6}$$

The overdot denotes the derivative of the quantity involved with respect to time, the superscript T refers to the total quantity, and the symbol $\perp$ denotes quantities perpendicular to the external magnetic field. It can be shown that because (μ,θ), (x_g, y_g), and (p_z, z) constitute the canonical set of variables, Eq. (5) follows directly from the continuity equation of the electron density in the six-dimensional space of the additional variables. Using the Krook model[24] the collisonal term on the right-hand side of Eq. (5) can be written as

$$\left[\frac{\partial F}{\partial t}\right]_{\rm collision} = -\nu_0(F - f_0^0) \ . \tag{7}$$

In the presence of the electromagnetic pump wave and electrostatic and electromagnetic decay waves, the total distribution function of electrons in Eq. (5) may be decomposed as

$$F = f_0^0 + f_0(\omega_0, \mathbf{k}_0) + f(\omega, \mathbf{k}) + f_1(\omega_1, \mathbf{k}_1) \ , \tag{8}$$

where the space and time variations are implied and the equilibrium distribution function f_0^0 is taken to be Maxwellian at the electron temperature T_e:

$$f_0^0 = n_0^0 \left[\frac{m}{2\pi T_e}\right]^{3/2} \exp\left[-\frac{mv^2}{2T_e}\right] . \tag{9}$$

f_0 and f_1 are high-frequency responses at the pump and the scattered sideband frequencies, respectively, and f is the low-frequency response. Using the equation of motions for electrons, we can write

$$\dot{\mu} = -\frac{e}{\omega_c}\mathbf{E}_\perp^T \cdot \mathbf{v}_\perp = -\frac{\partial H}{\partial \theta} \ , \tag{10}$$

$$\dot{\theta} = \frac{\partial H}{\partial \mu} = \omega_c - \frac{e}{mv_\perp}(E_x^T \sin\theta - E_y^T \cos\theta) \ , \tag{11}$$

$$\dot{\mathbf{x}}_g = \frac{e(\mathbf{E}_\perp^T \times \boldsymbol{\omega}_c)}{m\omega_c^2} \ , \tag{12}$$

$$H = \mu\omega_c + \frac{p_z^2}{2m} - e\Phi(\omega, \mathbf{k}) \ , \tag{13}$$

where

$$\Phi(\omega, \mathbf{k}) = \phi \exp[-i(\omega t - \mathbf{k}\cdot\mathbf{x})]$$

is the electrostatic potential of the low-frequency mode.

Using the identity

$$\exp[-i(\omega t - \mathbf{k}\cdot\mathbf{x})] \equiv \exp[-i(\omega t - \mathbf{k}\cdot\mathbf{x}_g)] \times \sum_n \exp[in(\theta - \delta)] J_n(k_\perp \rho) \ , \tag{14}$$

where J_n is the Bessel function of order n, and the summation over n runs form $-\infty$ to $+\infty$, we can express

$$\begin{aligned} \mathbf{E}^T = {} & \mathbf{E}_0' \exp[-i(\omega_0 t - k_0 x_g)] \sum_n \exp(in\theta) J_n^0 \\ & - i\mathbf{k}\phi \exp[-i(\omega t - \mathbf{k}\cdot\mathbf{x}_g)] \sum_n \exp[in(\theta - \delta)] J_n \\ & + \mathbf{E}_1' \exp[-i(\omega_1 t - \mathbf{k}_1 \cdot \mathbf{x}_g)] \sum_n \exp[in(\theta - \delta_1)] J_n^1 \ , \end{aligned} \tag{15}$$

$$F=f_0^0+\exp[-i(\omega_0 t-k_0 x_g)]\sum_n \exp(in\theta)f_n^0$$
$$+\exp[-i(\omega t-\mathbf{k}\cdot\mathbf{x}_g)]\sum_n \exp[in(\theta-\delta)]f_n$$
$$+\exp[-i(\omega_1 t-\mathbf{k}_1\cdot\mathbf{x}_g)]\sum_n \exp[in(\theta-\delta_1)]f_n^1 . \quad (16)$$

In Eqs. (14)–(16),

$$J_n=J_n(k_\perp\rho) ,$$
$$J_n^0=J_n^0(k_0\rho) ,$$
$$J_n^1=J_n^1(k_{1\perp}\rho) ,$$

and δ and δ_1 are the angles between the x axis and $\mathbf{k}_\perp$ and $\mathbf{k}_{1\perp}$, respectively. Using Eqs. (15) in Eqs. (10)–(13), we can write

$$\dot{\mu}=-\frac{eE_{0y}v_\perp}{\omega_c}(-i\beta_0\cos\theta+\sin\theta)\exp[-i(\omega_0 t-k_0 x_g)]\sum_n \exp(in\theta)J_n^0$$
$$-\frac{eE_{1y}v_\perp}{\omega_c}(-i\beta_1\cos\theta+\sin\theta)\exp[-i(\omega_1 t-\mathbf{k}_1\cdot\mathbf{x}_g)]\sum_n \exp[in(\theta-\delta)]J_n^1$$
$$+ie\phi\exp[-i(\omega t-\mathbf{k}\cdot\mathbf{x}_g)]\sum_n n\exp[in(\theta-\delta)]J_n , \quad (17)$$

$$\dot{\theta}=\omega_c+\frac{eE_{0y}}{mv_\perp}\left[-i\beta_0\sin\theta-\cos\theta+\frac{k_0 v_\perp}{\omega_0}\right]\exp[-i(\omega_0 t-k_0 x_g)]\sum_n \exp(in\theta)J_n^0$$
$$+\frac{e}{mv_\perp}\left[E_{1x}\sin\theta-E_{1y}\cos\theta+\frac{k_{1x}v_\perp}{\omega_1}E_{1y}\right]\exp[-i(\omega_1 t-\mathbf{k}_1\cdot\mathbf{x}_g)]\sum_n \exp[in(\theta-\delta_1)]J_n^1$$
$$-\frac{iek_\perp\cos\delta\,\sin\theta}{mv_\perp}\exp[-i(\omega t-\mathbf{k}\cdot\mathbf{x}_g)]\sum_n \exp[in(\theta-\delta)]J_n , \quad (18)$$

$$\dot{x}_g=\frac{eE_{0y}}{m\omega_c}\left[1-\frac{k_0 v_\perp\cos\theta}{\omega_0}\right]\exp[-i(\omega_0 t-k_0 x_g)]$$
$$\times\sum_n \exp(in\theta)J_n^0+\frac{eE_{1y}}{m\omega_c}\left[1-\frac{k_{1x}v_\perp\cos\theta}{\omega_1}\right]$$
$$\times\exp[-i(\omega_1 t-\mathbf{k}_1\cdot\mathbf{x}_g)]\sum_n \exp[in(\theta-\delta_1)]J_n^1 , \quad (19)$$

$$\dot{y}_g=\frac{eE_{0y}}{m\omega_c}\left[i\beta_0-\frac{k_0 v_\perp\sin\theta}{\omega_0}\right]\exp[-i(\omega_0 t-k_0 x_g)]\sum_n \exp(in\theta)J_n^0$$
$$-\frac{e}{m\omega_c}\left[E_{1x}+\frac{k_{1x}v_\perp\sin\theta}{\omega_1}E_{1y}\right]\exp[-i(\omega_1 t-\mathbf{k}_1\cdot\mathbf{x}_g)]\sum_n \exp[in(\theta-\delta_1)]J_n^1$$
$$+\frac{ie\phi k_1\cos\delta}{m\omega_c}\exp[-i(\omega t-\mathbf{k}\cdot\mathbf{x}_g)]\sum_n \exp[in(\theta-\delta)]J_n , \quad (20)$$

$$\dot{z}_g=\dot{z}=p_z/m$$
$$=-\frac{ek_0 E_{0y}v_z}{m\omega_0\omega_c}\exp[-i(\omega_0 t-k_0 x_g)]\sum_n \exp(in\theta)J_n^0$$
$$-\frac{ek_{1x}E_{1y}v_z}{m\omega_1\omega_c}\exp[-i(\omega_1 t-\mathbf{k}_1\cdot\mathbf{x}_g)]\sum_n \exp[in(\theta-\delta_1)]J_n^1 . \quad (21)$$

Using Eqs. (15)–(21) in the Boltzmann equation (5), we obtain the following linear response of electrons:

$$f_n^0=-\frac{eE_{0y}}{T_e}\frac{\beta_0\cos\theta+i\sin\theta}{\omega_0-n\omega_c+i\nu_0}v_\perp J_n^0 f_0^0 , \quad (22)$$

$$f_n^1=-\frac{ie}{T_e}\frac{E_{1x}\cos\theta+E_{1y}\sin\theta}{\omega_1-n\omega_c+i\nu_0}v_\perp J_n^1 f_0^0 , \quad (23)$$

$$f_n=-\frac{e\Phi}{T_e}\frac{n\omega_c}{\omega-n\omega_c+i\nu_0}J_n f_0^0 . \quad (24)$$

Substituting Eqs. (22)–(24) in Eq. (5), we obtain the nonlinear part of the distribution function for the low-frequency mode $(\omega,\mathbf{k})$ as

$$f_n^{\mathrm{NL}}=\frac{\exp(in\delta)}{(\omega-n\omega_c+i\nu_0)}\sum_l \exp[il(\theta-\delta_1)]\left[\frac{iek_{1x}E_{0y}}{2m\omega_c}\left[1-\frac{k_0v_\perp\cos\theta}{\omega_0}\right]J_n^0f_l^1 + \frac{iek_0E_{1y}}{2m\omega_c}\left[1-\frac{k_{1x}v_\perp\cos\theta}{\omega_1}\right]J_l^1f_n^0-\frac{iek_0k_{1z}E_{0y}}{2m\omega_0\omega_c}v_zJ_n^0f_l^1-\frac{eE_{0y}}{2\omega_c}(-i\beta_0\cos\theta+\sin\theta)v_\perp J_n^0\left[\frac{\partial f_l^1}{\partial\mu}\right] - \frac{e}{2\omega_c}(E_{1x}\cos\theta+E_{1y}\sin\theta)v_\perp J_l^1\left[\frac{\partial f_n^0}{\partial\mu}\right]+\frac{eE_{0y}}{2mv_\perp}\left[-i\beta_0\sin\theta-\cos\theta+\frac{k_0v_\perp}{\omega_0}\right]ilJ_n^0f_l^1 + \frac{e}{2mv_\perp}\left[E_{1x}\sin\theta-E_{1y}\cos\theta+\frac{k_{1x}v_\perp}{\omega_1}E_{1y}\right]inJ_l^1f_n^0\right] . \tag{25}$$

We obtain the linear and nonlinear density perturbation associated with the low-frequency electrostatic mode $(\omega,\mathbf{k})$ from the relation

$$n^{\mathrm{NL}}=\exp[-i(\omega t-\mathbf{k}\cdot\mathbf{x})]\int_{-\infty}^{\infty}\int_0^{2\pi}\int_0^{\infty}\sum_n \exp[in(\theta-\delta)]\exp\left[-\frac{ik_\perp v_\perp\sin(\theta-\delta)}{\omega_c}\right]f_n^{\mathrm{NL}}v_\perp dv_\perp d\theta\, dv_z . \tag{26}$$

Thus the linear and nonlinear density fluctuations at $(\omega,\mathbf{k})$ are given by

$$n^L=\sum_n \exp[-i(\omega t-\mathbf{k}\cdot\mathbf{x})]\frac{-n_0^0e\phi}{T_e}\frac{n\omega_c}{\omega-n\omega_c+i\nu_0}I_n(b)\exp(-b) , \tag{27}$$

$$n^{\mathrm{NL}}=\frac{\exp(-i\delta_1)\exp[-i(\omega t-\mathbf{k}\cdot\mathbf{x})]\omega_p^2E_{0y}(XE_{1x}+iYE_{1y})}{16\pi\sqrt{2\pi}T_ev_{\mathrm{th}}k_\perp^2\omega_0\omega_1(\omega_c-\omega-i\nu_0)} , \tag{28}$$

where

$$X=\exp(i\delta)(-\omega_0\omega_ck_{1x}+\omega_c^2k_\perp)+k_0k_{1x}k_\perp v_{\mathrm{th}}^2+\{i\omega_c(1-\beta_0)/2\}\{\omega_0(k_{1x}+4k_\perp)+\omega_1(k_0+4k_\perp)-ik_\perp\omega\} , \tag{29}$$

$$Y=\exp(i\delta)[\omega_0\omega_ck_{1x}-\omega_c^2k_\perp+\omega_1\omega_ck_0(1-\beta_0)]+k_0k_{1x}k_\perp v_{\mathrm{th}}^2(\beta_0-2) +\{i\omega_c(1-\beta_0)/2\}\{\omega_0(k_{1x}+4k_\perp)+\omega_1(k_0+4k_\perp)-i\omega k_\perp\} , \tag{30}$$

$$b=\left[\frac{k_\perp v_{\mathrm{th}}}{\omega_c}\right]^{1/2} ,$$

$$v_{\mathrm{th}}=\left[\frac{2k_BT_e}{m}\right]^{1/2} ,$$

and $I_n(b)$ is the modified Bessel function of the first kind and order n. In deriving Eq. (28) we have retained only the dominating terms having $(\omega-\omega_c+i\nu_0)$ in the denominators where $n=\pm1$.

For the high-frequency sideband, we use the fluid model of plasmas and obtain the nonlinear current density at $(\omega_1,\mathbf{k}_1)$ as

$$\mathbf{J}_1^{\mathrm{NL}}=-n^Lev_{0\perp}^*/2 =\frac{n_0^0e^3\phi\omega_c[\mathbf{E}_{0\perp}^*\times\boldsymbol{\omega}_c-(i\omega_0+\nu_0)\mathbf{E}_{0\perp}^*]}{2mT_e\sqrt{2\pi b}\,(\omega-\omega_c+i\nu_0)\{\omega_c^2+(\nu_0+i\omega_0)^2\}} , \tag{31}$$

where the asterisk (*) denotes the complex conjugate of the quantity involved.

III. NONLINEAR DISPERSION RELATION

Using Eq. (28) in Poisson's equation and in Eq. (31) in the wave equation for the high frequency-electromagnetic sideband, we obtain

$$\epsilon\Phi=-\left[\frac{4\pi e}{k^2}\right]n^{\mathrm{NL}} , \tag{32}$$

$$\overleftrightarrow{D}_1\cdot\mathbf{E}_1=\left[\frac{4\pi i\omega_1}{c^2}\right]\mathbf{J}_1^{\mathrm{NL}} , \tag{33}$$

where

$$\overleftrightarrow{D}_1=k_1^2\overleftrightarrow{I}-\mathbf{k}_1\mathbf{k}_1-\frac{\omega_1^2}{c^2}\overleftrightarrow{\epsilon}_1 , \tag{34}$$

$$\epsilon(\omega,\mathbf{k})=\epsilon_L+\frac{\omega_p^2(i\nu_0\omega+\omega^2-k^2v_{\mathrm{th}}^2)}{\omega_c^2\omega^2+(\nu_0\omega-i\omega^2+ik^2v_{\mathrm{th}}^2)^2} -\frac{K^2k^2C_s^2}{\omega^2-k^2C_s^2} , \tag{35}$$

and $\overleftrightarrow{I}$ is the unit tensor or rank 2. In Eq. (32), ϵ is the linear dielectric function of the low-frequency electrostatic perturbation.[5] The last term in the ϵ is the piezoelectric contribution from the lattice, where C_s is the ion-acoustic speed and K is the dimensionless electromechanical coupling coefficient. The numerical value of K^2 for most of the piezoelectric semiconductors[25] is $\sim 10^{-3}$. The dispersion relation of the electron acoustic wave is obtained from $\epsilon_r(\omega,\mathbf{k})=0$, where ϵ_r is the real part of the dielectric function given by Eq. (35). $\overleftrightarrow{\epsilon}_1$ in Eq. (34) is the linear dielectric tensor[10] at $(\omega_1,\mathbf{k}_1)$:

$$\overleftrightarrow{\epsilon}_1=\begin{vmatrix} \epsilon_L-\dfrac{i\omega_p^2(i\omega_1-\nu_0)}{\omega_1\{\omega_c^2+(\nu_0-i\omega_1)^2\}} & -\dfrac{i\omega_p^2}{\omega_c^2+(\nu^0-i\omega_1)^2}\dfrac{\omega_c}{\omega_1} & 0 \\ \dfrac{i\omega_p^2}{\omega_c^2+(\nu_0-i\omega_1)^2}\dfrac{\omega_c}{\omega_1} & \epsilon_L-\dfrac{i\omega^{p^2}(i\omega_1-\nu_0)}{\omega_1\{\omega_c^2+(\nu_0-i\omega_1)^2\}} & 0 \\ 0 & 0 & \epsilon_L+\dfrac{i\omega_p^2}{\omega_1(\nu_0-i\omega_1)} \end{vmatrix} .$$

Eliminating Φ and $\mathbf{E}_1$ between Eqs. (31) and (32), we obtain the nonlinear dispersion relation for the low-frequency perturbation as

$$\epsilon=\frac{\mu}{|\overleftrightarrow{D}_1|} , \tag{36}$$

where

$$|\overleftrightarrow{D}_1|=-\frac{\omega_1^2}{c^2}\left[\epsilon_L-\frac{\omega_p^2}{\omega_1^2}\right]\left\{k_1^2-\frac{\omega_1^2}{c^2}\left[\epsilon_L-\frac{\omega_p^2}{\omega_1^2}\right]\right\}^2-\frac{\omega_p^4\omega_c^2}{c^4\omega_1^2}\left\{k_{1x}^2-\frac{\omega_1^2}{c^2}\left[\epsilon_L-\frac{\omega_p^2}{\omega_1^2}\right]\right\} , \tag{37}$$

$$\mu=\frac{i|v_{0y}/v_{\rm th}|^2\omega_p^4\omega_c^2\omega_0\exp(-i\delta_1)Z}{4\pi k_\perp^3k^2v_{\rm th}^4c^2(\omega_c-\omega-i\nu_0)^2\{\omega_c^2+(\nu_0+i\omega_0)^2\}} , \tag{38}$$

$$\begin{aligned} Z=X&\left\{k_{1x}^2-\frac{\omega_1^2}{c^2}\left[\epsilon_L-\frac{\omega_p^2}{\omega_1^2}\right]\right\}\left[\left\{k_1^2-\frac{\omega_1^2}{c^2}\left[\epsilon_L-\frac{\omega_p^2}{\omega_1^2}\right]\right\}\{\omega_c-i\beta_0(i\omega_0+\nu_0)\}-\frac{i\omega_p^2\omega_c}{c^2\omega_1}\{i\beta_0\omega_c+(i\omega_0+\nu_0)\}\right] \\ &+Y\left[\frac{\omega_p^2\omega_c}{c^2\omega_1}\left\{k_{1x}^2-\frac{\omega_1^2}{c^2}\left[\epsilon_L-\frac{\omega_p^2}{\omega_1^2}\right]\right\}\{\omega_c-i\beta_0(i\omega_0+\nu_0)\}\right. \\ &\left.\quad-\frac{\omega_1^2}{c^2}\left[\epsilon_L-\frac{\omega_p^2}{\omega_1^2}\right]\left\{k_1^2-\frac{\omega_1^2}{c^2}\left[\epsilon_L-\frac{\omega_p^2}{\omega_1^2}\right]\right\}\{\beta_0\omega_c+(\omega_0-i\nu_0)\}\right] , \end{aligned} \tag{39}$$

$$|v_{0y}|=eE_{0y}/m\omega_0 ,$$

and X and Y are given by Eqs. (29) and (30).

IV. GROWTH RATES

To obtain the growth rate of the parametric instability, viz., the stimulated Brillouin scattering, we express ϵ and $|\overleftrightarrow{D}_1|$ around the resonant frequencies[22,23]

$$\omega=\omega_r+i\gamma ,$$

$$\begin{aligned} \epsilon(\omega,\mathbf{k})&=\epsilon_r+i\gamma\frac{\partial\epsilon_r}{\partial\omega}+i\epsilon_i \\ &\simeq i(\gamma+\gamma_L)\frac{\partial\epsilon_r}{\partial\omega} , \end{aligned} \tag{40}$$

$$|\overleftrightarrow{D}_1|\simeq i(\gamma+\gamma_L)\left[\frac{\partial|\overleftrightarrow{D}_1|_r}{\partial\omega_1}\right] , \tag{41}$$

where γ is the overall growth rate of the instability and γ_L and γ_{L1} are the linear damping rates of the decay waves, and the suffix r on ϵ and $|\overleftrightarrow{D}_1|$ denotes the real part, and $\epsilon_i=-\gamma_L(\partial\epsilon_r/\partial\omega)$ the imaginary part, of ϵ. Thus the growth rate of the three wave parametric instability is given by

$$(\gamma+\gamma_L)(\gamma+\gamma_{L_1})\equiv\gamma_0^2=-\frac{\mu}{(\partial\epsilon_r/\partial\omega)(\partial|\overleftrightarrow{D}_1|_r/\partial\omega_1)} , \tag{42}$$

where γ_0 is the growth rate in the absence of a damping of the waves. The linear damping rates of the electron-acoustic wave and the scattered laser radiation are given by[18,26]

$$\gamma_L=-\frac{\sqrt{2\pi}\nu_0K^2k^5v_{\rm th}^3C_s^2}{4\omega_p^2\omega\{(\omega_c-\omega)^2+\nu_0^2\}} , \tag{43}$$

$$\gamma_{L1}=-\frac{\omega_p^2(\nu_0+\omega_c)}{\epsilon_L\omega_0^2} . \tag{44}$$

Using Eqs. (35), (37), (38), and (42), we obtain the growth rate of the three wave parametric instability in the absence of the linear damping of the decay waves:

$$\gamma_0^2=\frac{i|v_{0y}/v_{\text{th}}|^2\omega_p^2\omega_c^4\omega^3\omega_0\exp(-i\delta_1)Z}{16\pi\epsilon_L k_1^3 k^4 v_{\text{th}}^6\omega_1(\omega_c-\omega-i\nu_0)^2\{\omega_c^2+(\nu_0+i\omega_0)^2\}P}, \tag{45}$$

where

$$P=\left\{k_1^2-\frac{\omega_1^2}{c^2}\left[\epsilon_L-\frac{\omega_p^2}{\omega_1^2}\right]\right\}\left\{k_1^2-\frac{3\omega_1^2}{c^2}\left[\epsilon_L-\frac{\omega_p^2}{\omega_1^2}\right]\right\} -\frac{\omega_p^4\omega_c^2}{\epsilon_L\omega_1^4c^2}\left[k_{1x}^2+\frac{\omega_p^2}{c^2}\right], \tag{46}$$

and Z is given by Eq. (39).

From Eq. (42) the overall growth rate γ in the presence of the linear damping of the decay waves can be obtained from

$$\gamma=[\{(\gamma_L+\gamma_{L1})^2+4(\gamma_0^2-\gamma_l\gamma_{L1})\}^{1/2} -(\gamma_L+\gamma_{L1})]/2, \tag{47}$$

and the threshold electric field for the onset of the instability can be obtained from

$$\gamma_0^2=\gamma_L\gamma_{L1}. \tag{48}$$

Now we consider two frequency regimes which are of practical interest.

A. High-frequency laser

For the high-frequency pump wave, viz., a CO_2 laser, we can take the approximations $\omega_0>\omega_p$, ω_c, ω, ν_0, and $k \gg k_0$, and for backscattering ($\delta_1=180^\circ$) the unperturbed growth rate γ_0. Equation (45) reduces to

$$\gamma_0\simeq\left[\frac{|v_{0y}/v_{\text{th}}|^2\omega_p^2\omega_c^4\omega^3}{16\pi\epsilon_L\omega_0(kv_{\text{th}})^6}\right]^{1/2}, \tag{49}$$

and the threshold power density of the incident laser radiation $P_0|_{\text{Th}}$ is given by

$$P_0|_{\text{Th}}=\frac{\sqrt{\pi}m^2cv_{\text{th}}^2\nu_0K^2(k^5C_s^2v_{\text{th}}^3)(kv_{\text{th}})^6\omega_0}{\sqrt{2}e^2\omega_p^2\omega_c^5\omega^4}. \tag{50}$$

B. Microwave radiation

For the microwave range of frequencies and for the typical parameters $\omega_0<\omega_p,\omega_c;\omega_c>\omega,\nu_0;\omega_0>\nu_0$, the growth rate and the threshold of the stimulated Brillouin scattering are given by

$$\gamma_0=\left[\frac{|v_{0y}/v_{\text{th}}|^2\omega_p^2\omega_c^2\omega^3\omega_0\beta_0}{16\pi\epsilon_L(kv_{\text{th}})^6}\right]^{1/2}, \tag{51}$$

$$P_0|_{\text{Th}}=\frac{\sqrt{\pi}m^2cv_{\text{th}}^2\nu_0K^2(k^5C_s^2v_{\text{th}}^3)(kv_{\text{th}})^6}{\sqrt{2}e^2\omega_p^2\omega_c^3\omega^4\omega_0\beta_0}. \tag{52}$$

V. NUMERICAL RESULTS AND GRAPHICAL REPRESENTATIONS

To gain some numerical appreciation of the results of our theory, we made calculations for the growth rates and threshold power densities for the stimulated Brillouin scattering for the following typical plasma parameters in n-InSb: $\epsilon_L=18$, $T_e=77$ K, $m=0.014m_0$ (m_0 is the mass of a free electron), $\nu_0=3.5\times10^{11}$ sec^{-1}, $\omega_p=2\times10^{13}$ sec^{-1}, $\omega_0=1.778\times10^{14}$ sec^{-1} (for a CO_2 laser) and 2×10^{12} sec^{-1} (for a typical microwave). The results of our calculations are depicted in the form of curves in Figs. 1 and 2.

Figure 1 shows variations of the growth rates of the stimulated Brillouin scattering as a function of the electron cyclotron frequency. It follows that the normalized growth rate of the three-wave parametric instability increases with the external uniform magnetic field. The undamped growth rate (γ_0/ω) of the stimulated Brillouin scattering is higher for the high-frequency pump wave than the microwave range of frequencies. However, the growth rate in the presence of damping (γ/ω) of the daughter waves is of the same order of magnitude.

Figure 2 shows the variation of the threshold power density of the instability as a function of electron cyclotron frequency. It is noticed that the threshold power density for the stimulated Brillouin scattering decreases rapidly with the increase of magnetic field.

It is observed from comparison of our results with those of Guha and Basu[18] that the growth rate of the instability leading to the stimulated Brillouin scattering increases with magnetic field, which is in clear contrast with their results. It is also noticed that our calculation

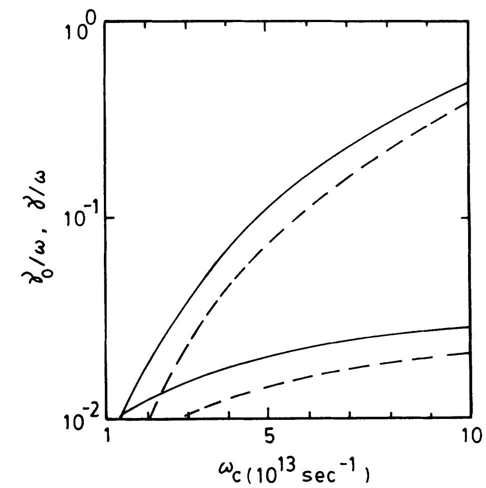

FIG. 1. Variation of unperturbed normalized growth rate, γ_0/ω, and overall normalized growth rate, γ/ω, with ω_c for the following parameters in n=InSb: $\epsilon_L=18$ (at 77 K), $K^2=10^{-3}$, $\nu_0=3.5\times10^{11}$ sec^{-1}, $k=10^6$ cm^{-1}, $\omega_p=2\times10^{13}$ sec^{-1}, $m/m_0=0.014$, $C_s=4\times10^5$ cm/sec, and $|v_{0y}/v_{\text{th}}|=|eE_{0y}/m\omega_0v_{\text{th}}|=10^{-3}$. The solid curves represent γ_0/ω, while the dashed curves represent γ/ω. The upper curves are for $\omega_0=1.778\times10^{14}$ sec^{-1}, and the lower curves are for $\omega_0=2\times10^{12}$ sec^{-1}.

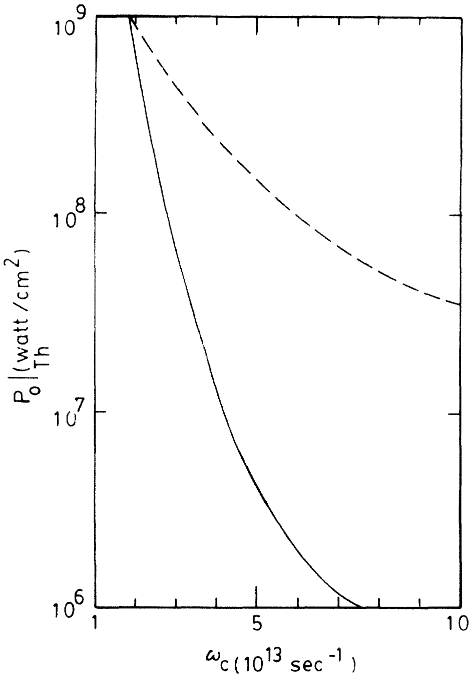

FIG. 2. Variation of the threshold power density of the incident wave, $P_0|_{\rm Th}$, with ω_c for the parameters as in Fig. 1. The solid curve is for $\omega_0 = 1.778\times10^{14}$ sec^{-1}, and the dashed curve is for $\omega_0 = 2\times10^{12}$ sec^{-1}.

of the stimulated Brillouin scattering for laser radiation yields growth rate approximately one order higher than that calculated from the fluid model.[18] This discrepancy may be attributed to the correct model of the semiconductor plasma.

VI. DISCUSSION

It has been shown that a large-amplitude electromagnetic wave propagating in the extraordinary mode decays efficiently exciting an electron acoustic wave and a scattered electromagnetic sideband in a magnetized semiconductor plasma. It is noticed [cf. Eq. (49)] that the growth rate of the stimulated Brillouin scattering of high-frequency laser radiation is directly proportional to the pump-induced drift velocity of electrons. It increases with the plasma density and increases rapidly with the increase of the external magnetic field. γ_0 is a sensitive function of the electron temperature of the semiconductor, and decreases sharply with an increase of temperature. The linear damping rates γ_L and γ_{L1} are small for the usual plasma parameters. Hence the threshold power density of the incident pump wave [cf. Eq. (50)] is small. However, it increases sharply with temperature and decreases with an increase of the external magnetic field. We also observe [cf. Eqs. (51) and (52)] that for the microwave range of frequencies for the pump wave the growth rate γ_0 increases rather slowly with the external magnetic field, and the threshold power density decreases relatively slowly with the external magnetic field in comparison with those at the high-frequency pump wave.

Our results differ from those of Guha and Basu[18] in one important respect: the growth rate of the stimulated Brillouin scattering increases with an increase of the external static magnetic field for the short-wavelength perturbation in the n-type semiconductor plasma. It is observed from comparison of our results with those of Guha and Basu[18] that the growth rate of the instability leading to the stimulated Brillouin scattering increases with the magnetic field, which is in clear contrast with their results. It is also noticed that our calculation of the stimulated Brillouin scattering for the laser radiation yields a growth rate approximately one order higher than that calculated using the fluid model.[18] This may be due to the fact that the correct kinetic model of plasmas must be employed instead of the hydromagnetic model of the semiconductor plasmas for studies of the parametric instability for the very short-wavelength perturbation mode. The results of this paper also suggest that various aspects of the parametric instabilities can be verified experimentally in a semiconductor where the plasma parameters can be conveniently varied over a wide range of values without much difficulty.

ACKNOWLEDGMENT

The authors are thankful to Dr. M. Ruhul Amin for useful discussions at the final stage of the manuscript.

[1]W. Beer, in *Semiconductor and Semimetals,* edited by R. R. Willardson (Academic, New York, 1966), Vol. 1, p. 417.

[2]S. J. Buchsbaum and P. M. Platzman, Phys. Rev. **154**, 395 (1967).

[3]J. R. Houck and R. Bowers, Phys. Rev. **166**, 397 (1968).

[4]H. Hartnagel, *Semiconductor Plasma Instabilities* (Heinemann, London, 1969).

[5]M. C. Steele and B. Vural, *Wave Interactions in Solid State Plasmas,* Advanced Physics Monograph Series (McGraw-Hill, New York, 1969).

[6]Juras Pozhela, *Plasma and Current Instabilities in Semiconductors* (Pergamon, New York, 1981).

[7]N. Bloembergen, *Nonlinear Optics* (Benjamin, New York, 1965).

[8]G. C. Baldwin, *An Introduction to Nonlinear Optics* (Plenum, New York, 1969).

[9]S. A. Akhmanov and R. V. Khokhlov, *Problems of Nonlinear Optics* (Gordon and Breach, New York, 1972).

[10]M. S. Sodha, A. K. Ghatak, and V. K. Tripathi, Prog. Opt. **13**, 169 (1976).

[11]S. Guha, P. K. Sen, and S. Ghosh, Phys. Status Solidi B **91**, K135 (1979).

[12]Y. K. Pozhela, R. B. Tolutis, and Z. K. Yankanshas, Radiophys. Quantum Electron. **27**, 552 (1984).

[13]M. Longtin and B. U. O. Sonnerup, J. Geophys. Res. **91**, 681 (1986).
[14]L. Stenflo and P. K. Shukla, Phys. Rev. B **39**, 12941 (1989).
[15]M. Salimullah, S. M. Khurshed Alam, and M. N. Alam, Phys. Rev. B **39**, 3771 (1989).
[16]V. E. Gusev, Phys. Status Solidi B **158**, 367 (1990).
[17]P. Aghamkar and P. K. Sen, Phys. Status Solidi B **157**, 735 (1990).
[18]S. Guha and C. Basu, Phys. Status Solidi B **122**, 799 (1984).
[19]S. Guha, C. Basu, and M. Bose, Phys. Status Solidi A **83**, 675 (1984).
[20]S. Guha and C. Basu, Phys. Status Solidi B **127**, K137 (1985).
[21]R. E. Aamodt, Y. C. Lee, C. S. Liu, and M. N. Rosenbluth, Phys. Rev. Lett. **39**, 1660 (1977).
[22]C. S. Liu and V. K. Tripathi, Phys. Rep. **130**, 143 (1986).
[23]C. S. Liu and P. K. Kaw, in *Advances in Plasma Physics*, edited by A. Simon and W. B. Thompson (Wiley, New York, 1976), Vol. VI, p. 83.
[24]D. R. Nicholson, *Introduction to Plasma Theory* (Wiley, New York, 1983).
[25]K. Seeger, *Semiconductor Physics* (Springer-Verlag, Wien, 1973).
[26]R. R. Sharma and V. K. Tripathi, Phys. Rev. B **20**, 748 (1979).